

RESEARCH

Open Access

An instrument design for non-contact detection of biomolecules and minerals on Mars using fluorescence

Heather D Smith^{1,2*}, Christopher P McKay², Andrew G Duncan³, Ronald C Sims¹, Anne J Anderson⁴ and Paul R Grossl⁵

Abstract

We discuss fluorescence as a method to detect polycyclic aromatic hydrocarbons and other organic molecules, as well as minerals on the surface of Mars. We present an instrument design that is adapted from the ChemCam instrument which is currently on the Mars Science Lander Rover *Curiosity* and thus most of the primary components are currently flight qualified for Mars surface operations, significantly reducing development costs. The major change compared to ChemCam is the frequency multipliers of the 1064 nm laser to wavelengths suitable for fluorescence excitation (266 nm, 355 nm, and 532 nm). We present fluorescence spectrum for a variety of organics and minerals relevant to the surface of Mars. Preliminary results show minerals already known on Mars, such as perchlorate, fluoresce strongest when excited by 355 nm. Also we demonstrate that polycyclic aromatic hydrocarbons, such as those present in Martian meteorites, are highly fluorescent at wavelengths in the ultraviolet (266 nm, 355 nm), but not as much in the visible (532 nm). We conclude that fluorescence can be an important method for Mars applications and standoff detection of organics and minerals. The instrument approach described in this paper builds on existing hardware and offers high scientific return for minimal cost for future missions.

Introduction

A practical difficulty with organic and biological analysis on Mars missions is getting to, and collecting, the sample. Rovers remotely operated from Earth can take many days to drive to a site and to collect a sample. For this reason there is considerable interest in selection of target samples – both rock and dirt - from a distance of several meters.

The current method for non-contact detection on the *Mars Science Laboratory* (MSL) is *ChemCam*. *ChemCam* employs Laser-Induced Breakdown Spectrometer (LIBS) and can accomplish elemental chemical determination [1]. *ChemCam* consists of two instruments: 1) a remote micro-imager (RMI) capable of mm resolution from meters away and 2) a laser-induced breakdown spectrograph (LIBS) capable of determining certain elemental concentrations as low as 10 ppm [1]. The *ChemCam*

instrument sits on the *Curiosity* rover mast 1.8 meters above the ground allowing for remote analysis at distances up to 9 meters [1]. The *ChemCam* instrumentation has achieved several technical breakthroughs including the first flight-qualified laser. All of the *ChemCam* hardware, including the excitation and emission systems, have achieved flight qualification, and are at Technical Readiness Level (TRL) 9 now that MSL is operating on the martian surface. A major addition in standoff detection would be the ability to detect low levels (ppm and less) of organics in rock and soil samples. Two methods are under consideration for this task: Raman spectroscopy and UV fluorescence. Standoff detection of organics by both Raman [2,3] and fluorescence [4] have been demonstrated in laboratory trials. In general, Raman spectroscopy provides better identification of organics than fluorescence while fluorescence provides a higher sensitivity to low levels of organics. In this paper we focus on fluorescence as a method to do stand-off detection of biological, organic, and mineralogical assays on future Mars missions.

* Correspondence: hdsmith@aggiemail.usu.edu

¹Department of Biological Engineering, Utah State University, Logan, UT, USA

²NASA Ames Research Center, Space Science Division, Moffett Field, CA, USA

Full list of author information is available at the end of the article

Characterization of targets via fluorescence involves both an excitation wavelength and an emission wavelength. The excitation that results in fluorescence occurs when a photon of the appropriate wavelength reaches, or excites, the target and the energy state of an electron is raised. As the energy dissipates, the electron cascades down to lower energy states. The energy released in this cascade is emitted as photons of wavelengths longer than the excitation wavelength due to the loss of energy required to raise the electron state.

Previous investigations have employed the use of native fluorescence for mineral identification, organics, and photosynthetic compounds for over 100 years [5-16]. One such investigation examined using native fluorescence spectra of chlorophyll a and other photosynthetic pigments in their natural environment using airborne assets was first reported by Hoge and Swift [5]. A more extensive investigation using various pigment-protein Macromolecules in the 480–560 spectral region demonstrated the capability of measuring a variety of photosynthetic pigments using native fluorescence [6]. More recent investigations measured the fluorescence of several photosynthetic pigments to determine the microbial community of photosynthetic organisms [15,16]. A few in-situ fluorescence instruments have been developed to identify bio-signatures and are at various stages of flight technical readiness levels. These instruments are aimed at detecting microbes by adding a fluorescing reagent [17] or within a fairly uniform, low fluorescence material such as ice [18,19] and in the ocean [20]. Work has begun to look at native fluorescence in soil as well [21]. These instruments provide a fluorescent method for detecting biomolecules and chemical organics.

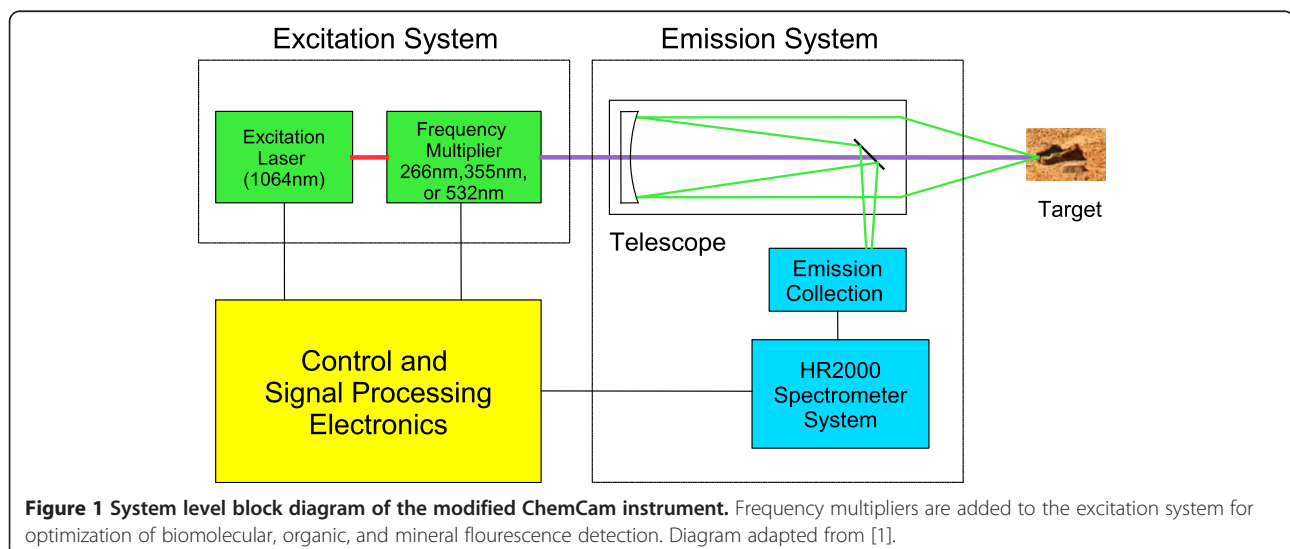
In addition to detecting biomolecules and chemical organics, fluorescence can also be used as a tool for

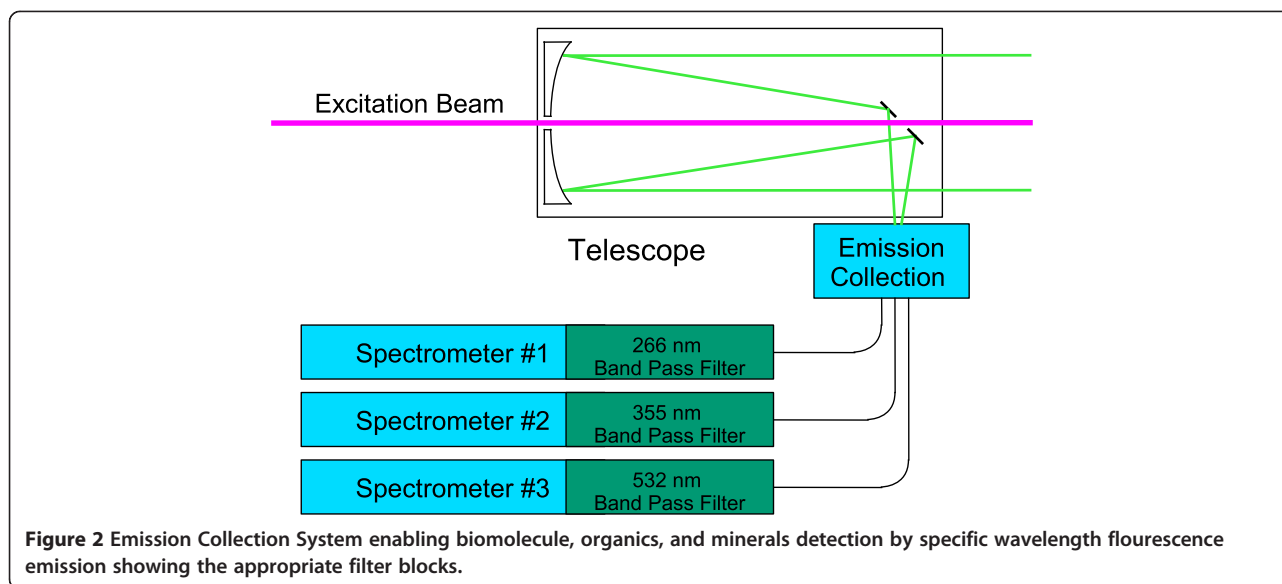
mineralogical identification [22] to aid in target selection. Many minerals are fluorescent when excited at certain excitation and emission wavelength combinations, for example, the mineral fluorite derives its name after this characteristic fluorescence property. Often in planetary applications spectral information requires information on the geological context before a mineral is identified. This does not diminish the utility of spectral data. Mineral and rock species identified on the surface of Mars include hematite, jarosite, olivine, phyllosilicates, carbonates, perchlorate (ClO_4), basalts, and ice among others [23,24].

Modified ChemCam Instrument

The LIBS system that forms the core of ChemCam is a suitable starting point for future combined LIBS/Raman or LIBS/fluorescence instruments. Laser induced breakdown spectroscopy operates by heating/energizing the target surface producing a plasma. Elements are identified and their concentration determined based on the strength of atomic emission lines in the spectrum. ChemCam uses a 5 ns pulsed 1064 nm laser with a 15 hz firing rate drawing 30 mJ per pulse to produce the plasma [1]. To capture the emission spectrum of the plasma, ChemCam has a Schmidt telescope to increase the light gathering power before feeding the signal into three spectrometers. The spectrometers are customized versions of off-the-shelf Ocean Optics HR2000 spectrometers, each designed to measure specific wavelengths of the emission spectra (240–336 nm, 380–470 nm, 500–800 nm respectively). In a typical application the signal is integrated over 75 laser pulses. The combined spectrometer detection ranges from ultra-violet (UV) 240 nm to red 800 nm [1].

The primary component of the ChemCam instrument that enables fluorescence assessment is the 1064 nm laser. This wavelength (1064 nm) is too long of a wavelength,





hence too low-energy to induce fluorescence. However with the aid of a frequency multiplier, irradiation can be produced at the three harmonic wavelengths, double, triple, and quadruple of the frequency of the original 1064 nm light, corresponding to wavelengths of 532 nm, 355 nm, and 266 nm, respectively. Biological material, organics, and minerals fluoresce when excited at 266 nm and 355 nm. Thus the main modification of the ChemCam excitation system to enable fluorescence is the addition of three interchangeable frequency multipliers. A flight-

qualified mechanical drive train and control box used for the camera filter wheel, for example that used on board the *Beagle 2 Lander* [25,26] could rotate the frequency multipliers into position. Figure 1 is a system level block diagram of the new instrument.

The emission collection system has one main modification, the placement of a band pass notch filter in front of each of the three spectrometers. These filters block the excitation wavelengths allowing the natural fluorescence to pass through to the spectrograph. The emission collection

Table 1 Common organics (polycyclic aromatic hydrocarbons, PAH) of extraterrestrial origin (meteorites, interstellar medium (ISM)), and potential biomolecules that could be on the surface of Mars, excitation and emission wavelength peaks, and reference

Biomolecules	Description	Excitation λ	Emission λ	Reference
ATP	ubiquitous metabolite	280 nm	420 nm	Katayama et al. [30]
Phenylalanine	amino acid in ISM	260 nm	282 nm	Seaver et al. [31]
NADH	ubiquitous metabolite	350 nm	460 nm	Richards-Kortum et al. [32]
Tyrosine	amino acid in ISM	275 nm	304 nm	Nevin et al. [33]
Tryptophan	amino acid in ISM	280 nm	353 nm	Alimova et al. [34]
Chemical organics				
Benzopyrene	PAH in Mars meteorites	383 nm	435 nm	Kuijt et al. [35]
Chrysene	PAH in Mars meteorites	307 nm	370 nm	Kuijt et al. [35]
Napthalene	PAH in Mars meteorites	275 nm	344 nm	Kuijt et al. [35]
Perylene	PAH in Mars meteorites	280 nm	no peak	Pujari et al. [36]
Perylene		440 nm	472 nm	Wilson et al. [37]
Phenanthrene	PAH in Mars meteorites	280 nm	410 nm	Pujari et al. [36]
Phenanthrene		306 nm	361 nm	Kuijt et al. [35]
Pyrene	PAH in Mars meteorites	347 nm	387 nm	Kuijt et al. [35]
Pyrene		342 nm	376, 396 nm	Wilson et al. [37]

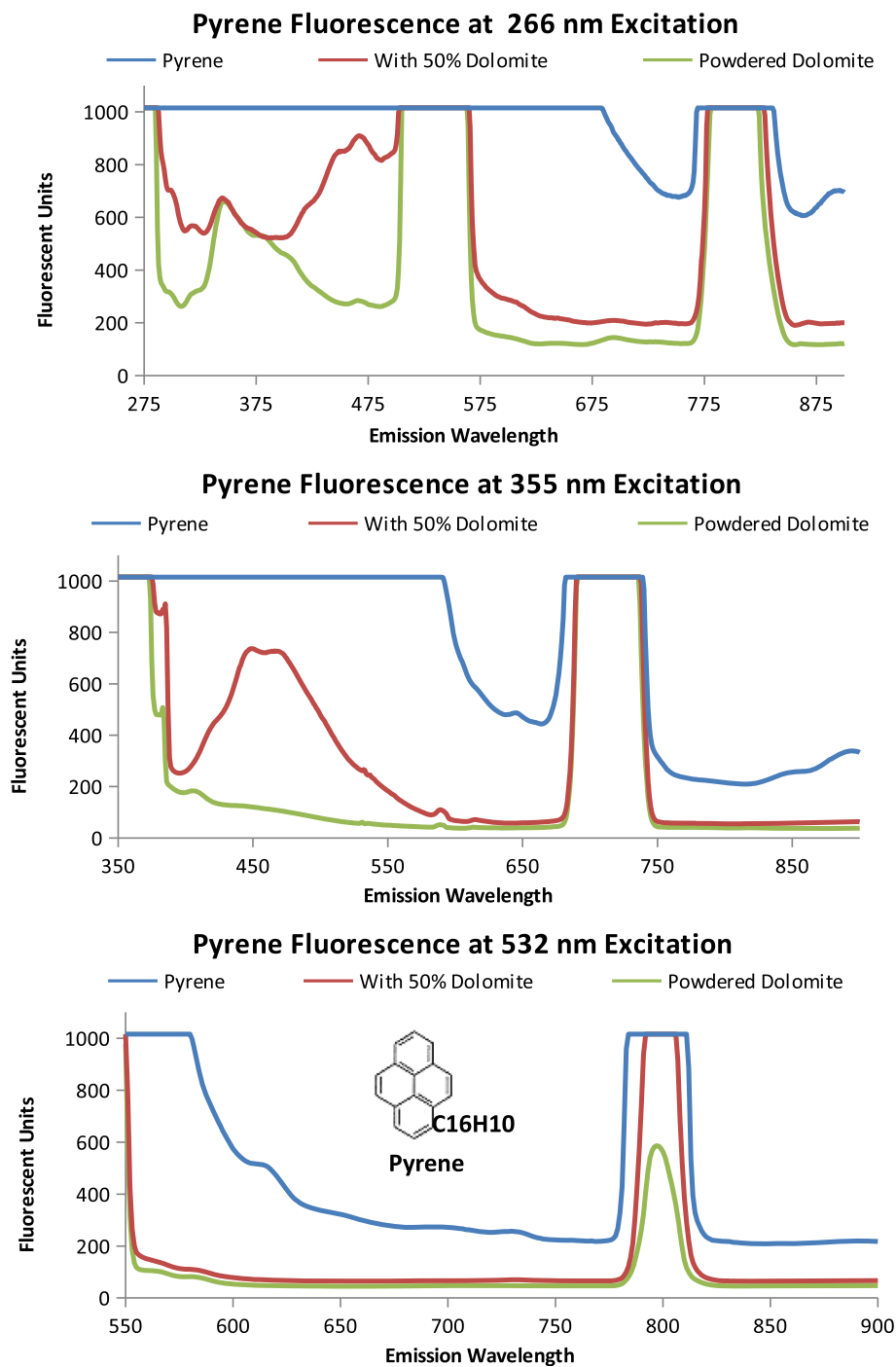


Figure 3 Pyrene Fluorescence. Each graph is the emission spectra of pyrene, powdered dolomite, and a 50/50 by volume mixture of dolomite and pyrene when excited at proposed excitation wavelengths (266 nm, 355 nm, and 532 nm). The molecular structure and formula is shown on the 532 nm emission graph.

system (Figure 2) will employ the Schmidt telescope, the original three ChemCam spectrographs, and the addition of three notch narrow band pass filters (266 nm, 355 nm, and 532 nm). The only non-flight qualified hardware of the entire fluorescence instrument design are the

frequency multipliers and the non-moving band pass notch filters as every other system component has been flight qualified. An estimate of these additional components is less than a kilogram of mass and in the tens of thousands of dollars.

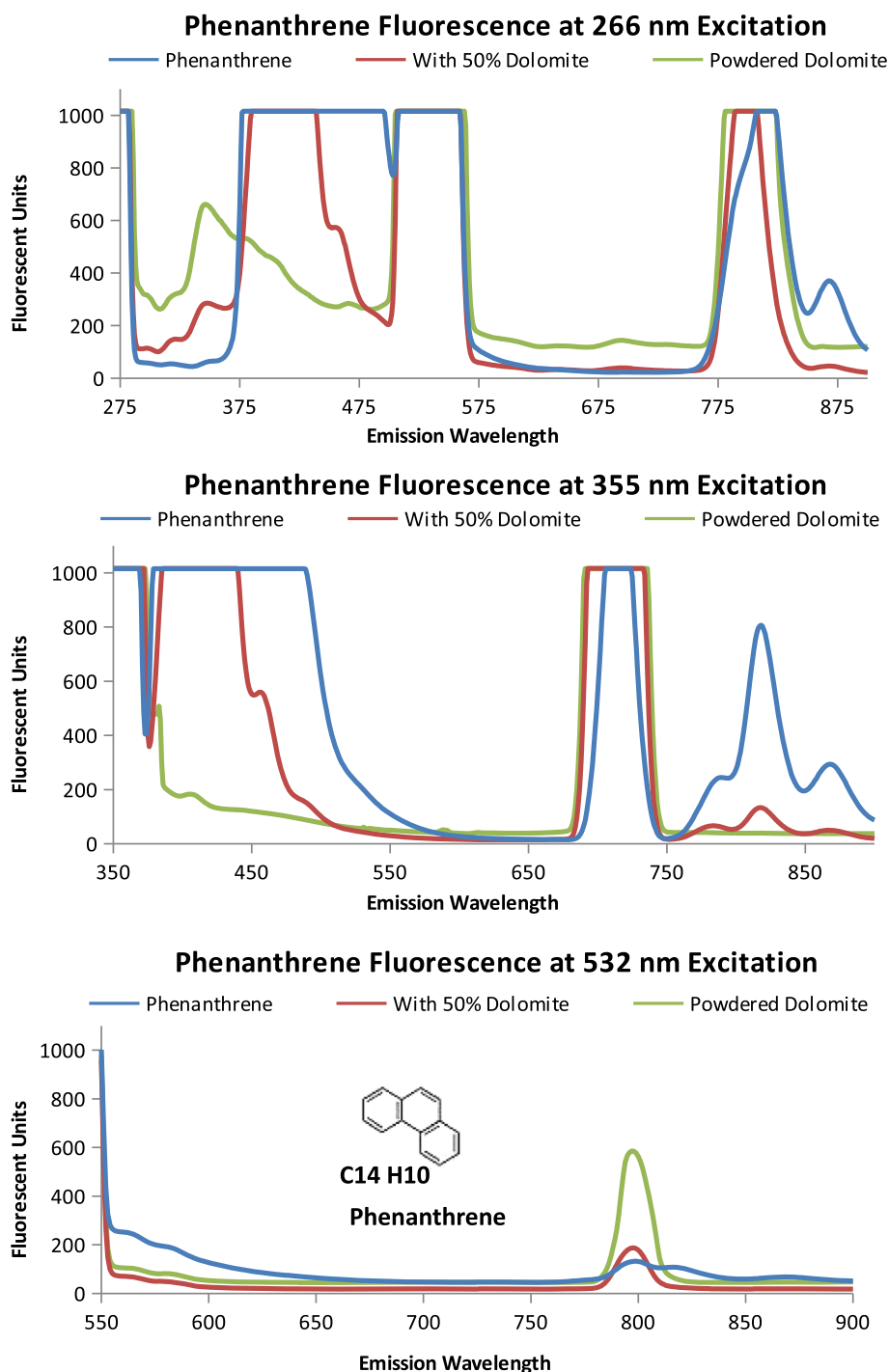


Figure 4 Phenanthrene Fluorescence. Emission Spectra of phenanthrene, powdered dolomite, and a 50/50 by volume mixture of dolomite and phenanthrene when excited at proposed excitation wavelengths (266 nm, 355 nm, and 532 nm). The molecular structure and formula is shown on the 532 nm emission graph.

UV fluorescence of organics and minerals relevant to Mars
 Many organic molecules, particularly polycyclic aromatic hydrocarbons (PAHs) fluoresce (See Table 1). Polycyclic aromatic hydrocarbons have been found in Martian

meteorites, and are the primary form of organic matter found in many meteorites [27]. Biomolecules occurring as amino acids have been detected in the interstellar medium (ISM) [28]. Hence, PAHs and amino acids are plausible

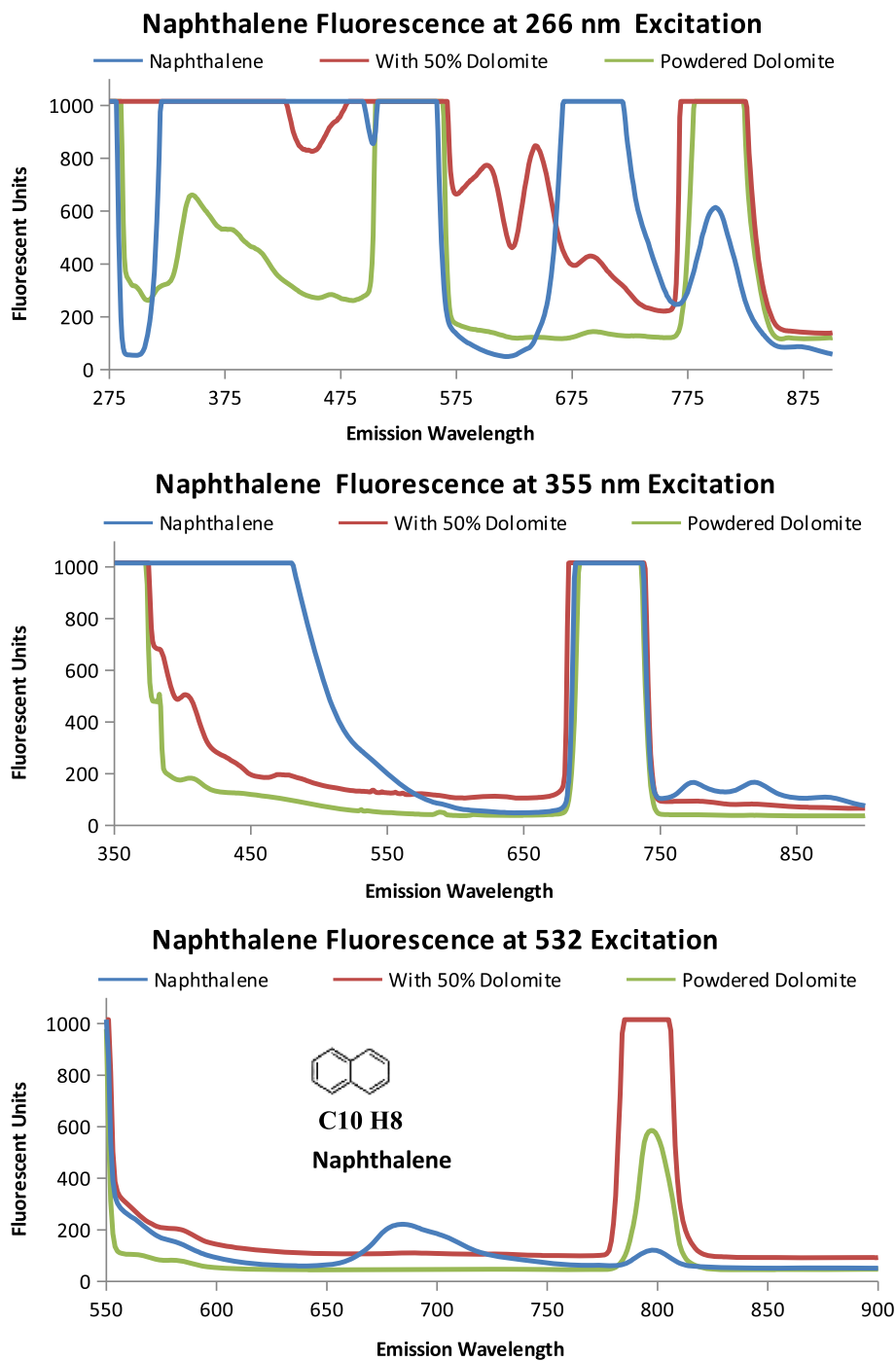


Figure 5 Naphthalene Fluorescence. Emission Spectra of naphthalene powdered dolomite, and a 50/50 by volume mixture of dolomite and naphthalene when excited at proposed excitation wavelengths (266 nm, 355 nm, and 532 nm). The molecular structure and formula is shown on the 532 nm emission graph.

candidates for organics on Mars. Storrie-Lombardi et al. [4] detected fluorescence, using a camera and filter wheel, of the three- ring-PAH anthracene, the four ring pyrene, and the five-ring perylene when excited at 365 nm. The fluorescence characteristics of several PAH's are listed in

Table 1. Also listed are the fluorescent characteristics of the aromatic amino acids, phenylalanine, tyrosine, and tryptophan. In addition other biomolecules can be detected and identified using fluorescence as shown for ATP and NADH in Table 1. For a more detailed list

of fluorescence of common biomolecules and detection of biomolecules by fluorescence refer to the Additional file 1 which is based on Smith et al. [29].

Methods

To ascertain fluorescence response at the constrained excitation wavelengths (266 nm, 355 nm, and 532 nm), we measured the emission spectra for five PAHs (pyrene, phenanthrene, naphthalene, naphthol, and cresol) individually and when combined with a mineral in a 50/50 mixture by volume. The polycyclic aromatic hydrocarbons, (pyrene, phenanthrene, naphthalene, cresol, and naphthol), powdered dolomite, and Ca perchlorate were purchased from Sigma Aldrich (St. Louis, MO). Powdered dolomite was used as the mineral since it is a magnesium carbonate formed under aqueous conditions and possibly on the Martian surface [23].

Even though the primary task of the fluorescence instrument is to identify organics, the identification of minerals, especially water-associated minerals, would enhance the scientific value without adding to the cost.

To determine the feasibility of identifying minerals using the fluorescence instrument, emission spectra of several rock minerals known to be on the surface of Mars were generated for each of the three excitation wavelengths proposed for this instrument. Additionally emission spectra for rock minerals found at Mars Analog environments on Earth and potentially on Mars were measured. The rock mineral specimens (except for jarosite) were from the Utah State University Geology Department mineralogy and igneous petrology collection. Jarosite was collected from Panoche Valley in California by the research team.

All of the data presented in this paper were taken with a Shimadzu RF-1501 Fluorometer set to a resolution of 5 nm. This instrument has a wavelength accuracy of ± 1.5 nm and a signal to noise ratio of 150:1 [38]. Our standard deviation based on triplicate sample measurements is less than 1%, therefore we suggest the inhomogeneity of a sample could introduce a greater error than the that introduced by the method. A custom angled

cuvet for powdered mixtures and a sample holder able to hold rocks was positioned in the fluorometer to obtain optimal emission spectra. Each specimen was excited by the fluorometer xenon flash lamp, at 266 nm, 355 nm, and 532 nm and the emission spectra scanned from 220–900 nm, 350–900 nm, and 530–900 nm respectively.

Results

Fluorescence and quenching results for three polyaromatic hydrocarbons likely to be on Mars, pyrene, phenanthrene, and naphthalene, are shown in Figures 3, 4, and 5 and described in Table 2. The emission spectra for the individual PAH is compared with a 50% PAH 50% powdered dolomite by volume mixture and the spectrum for powdered dolomite.

The fluorescence from pyrene is shown in Figure 3. As shown in Figure 3A, when excited at 266 nm pyrene saturates the instrument detectors causing a flat line at the highest instrument readings (1000 Fluorescent units). The powdered dolomite and the 50/50 mixture of pyrene and dolomite have an emission peak at 340 nm. This dolomite peak at 340 nm was also seen in the 50/50 mixture of pyrene and dolomite. The addition of the dolomite quenched the pyrene signal by lowering the fluorescent units to 600 for the 50% pyrene, 50% dolomite mixture compared with over 1000 fluorescent units for pyrene alone. Rather than fluorescence, the peaks from 498 to 532 nm, and the peak from 770 to 810 nm are likely due to instrumentation setup and interactions between the excitation wavelength and the samples analyzed (dolomite and pyrene) which produces a resonance frequency at two times the excitation wavelength (2λ , $2 \times 266 = 532$ nm). Resonance frequencies can also occur at other intervals such as three times the excitation wavelength ($3\lambda = 798$ nm) as seen in the peak between 770 and 810 nm. As seen in Figure 3B with the 355 nm excitation, the fluorescence emission detectors are saturated until 590 nm where the fluorescence sharply drops to around 500 fluorescent units and continues to reduce. The 710 nm emission peak (2λ) should be regarded as an artifact of the spectrometer grating instead of fluorescence. The 440 nm emission from the 50%

Table 2 Summary of PAH spectrum characteristics for each of the polycyclic aromatic hydrocarbons shown above as measured for this study using a Shimadzu 1501 Fluorometer

PAH	266 nm ex spectrum comparison		355 nm ex spectrum comparison		532 nm ex spectrum comparison	
	Fluorescence(nm)	Quenching(nm)	Fluorescence (nm)	Quenching (nm)	Fluorescence (nm)	Quenching (nm)
Pyrene	260 to 650		355 to 590		532 to 590	
Phenanthrene	352 to 500, 861	291 to 351, 501	377 to 507, 818	376	550 to 650	
Naphthalene	315 to 557, 640 to 740	291 to 314 558 to 640	355 to 506, 766, 818		683	
Naphthol	321 to 400	291 to 320	410			790
Cresol	380		355 to 450, 770	710		790

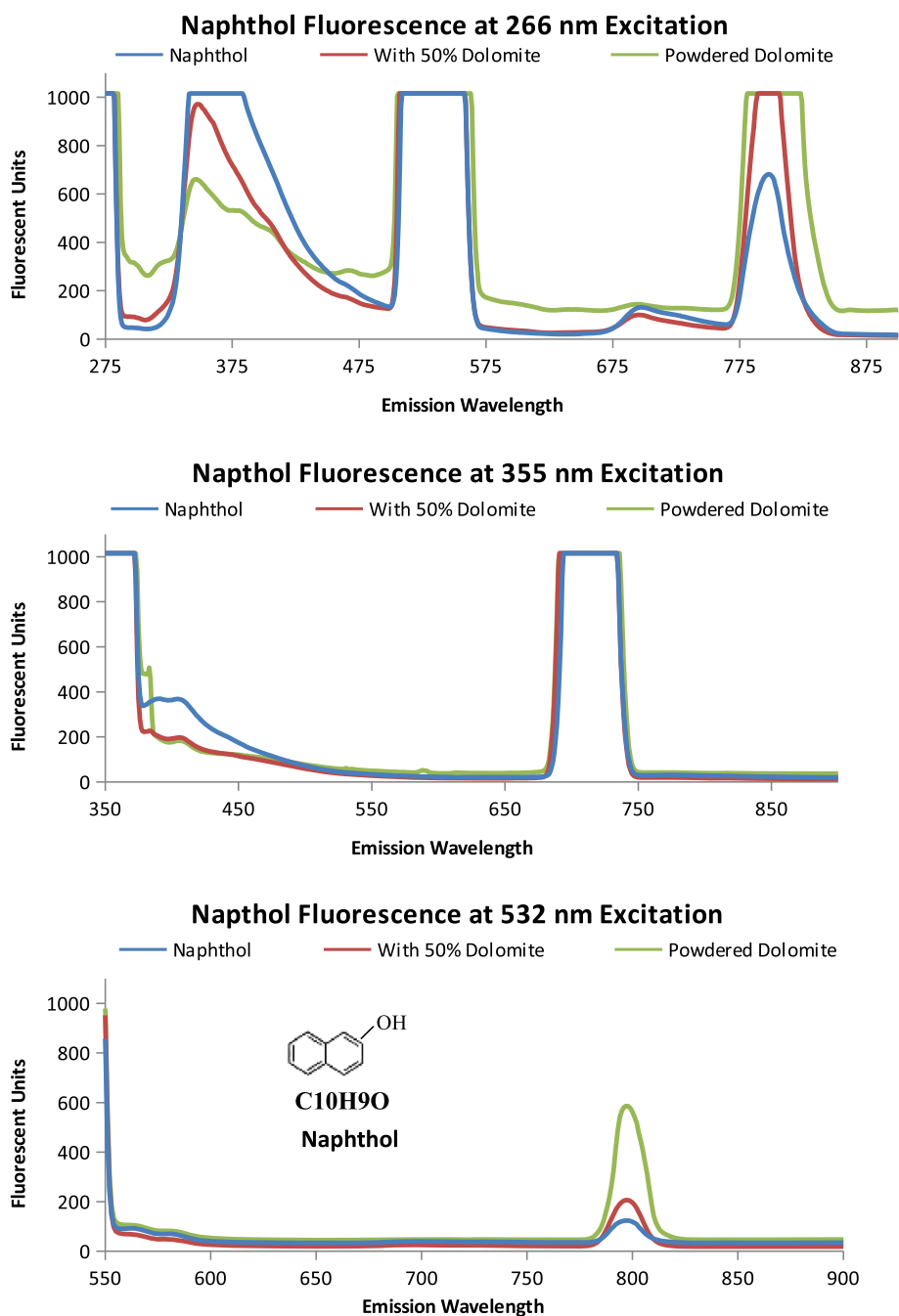


Figure 6 Naphthol Fluorescence. Emission spectra of naphthol, powdered dolomite, and a 50/50 mix when excited excitation wavelengths 266 nm, 355 nm, and 532 nm. The molecular structure and formula is shown on the 532 nm emission graph.

pyrene to 50% dolomite mixture by volume both enhances the dolomite peak at 440 nm and reduces the pyrene emission. For pyrene, as the excitation energy decreases, so does the variation in emission spectra (from graphs 3A to 3C). In 3C, when excited at 532 nm, pyrene has a small emission peak at 615 nm. The peak at 790 nm (1.5 λ) frequency resonance is less for dolomite than for pyrene, and the 50% pyrene 50% dolomite by volume mixture.

In Figure 4 the three-ringed phenanthrene displays distinguishing emission spectra at each excitation wavelength. In Figure 4A, only phenanthrene has an emission peak at 861 nm (266 nm ex) and fluoresces from 351 to 500 nm. At 355 nm excitation the 50% phenanthrene 50% dolomite by volume mixture and phenanthrene both have an emission peak at 818 nm. When Phenanthrene is excited at 532 nm, the 818 nm peak seen at 355 excitation disappears.

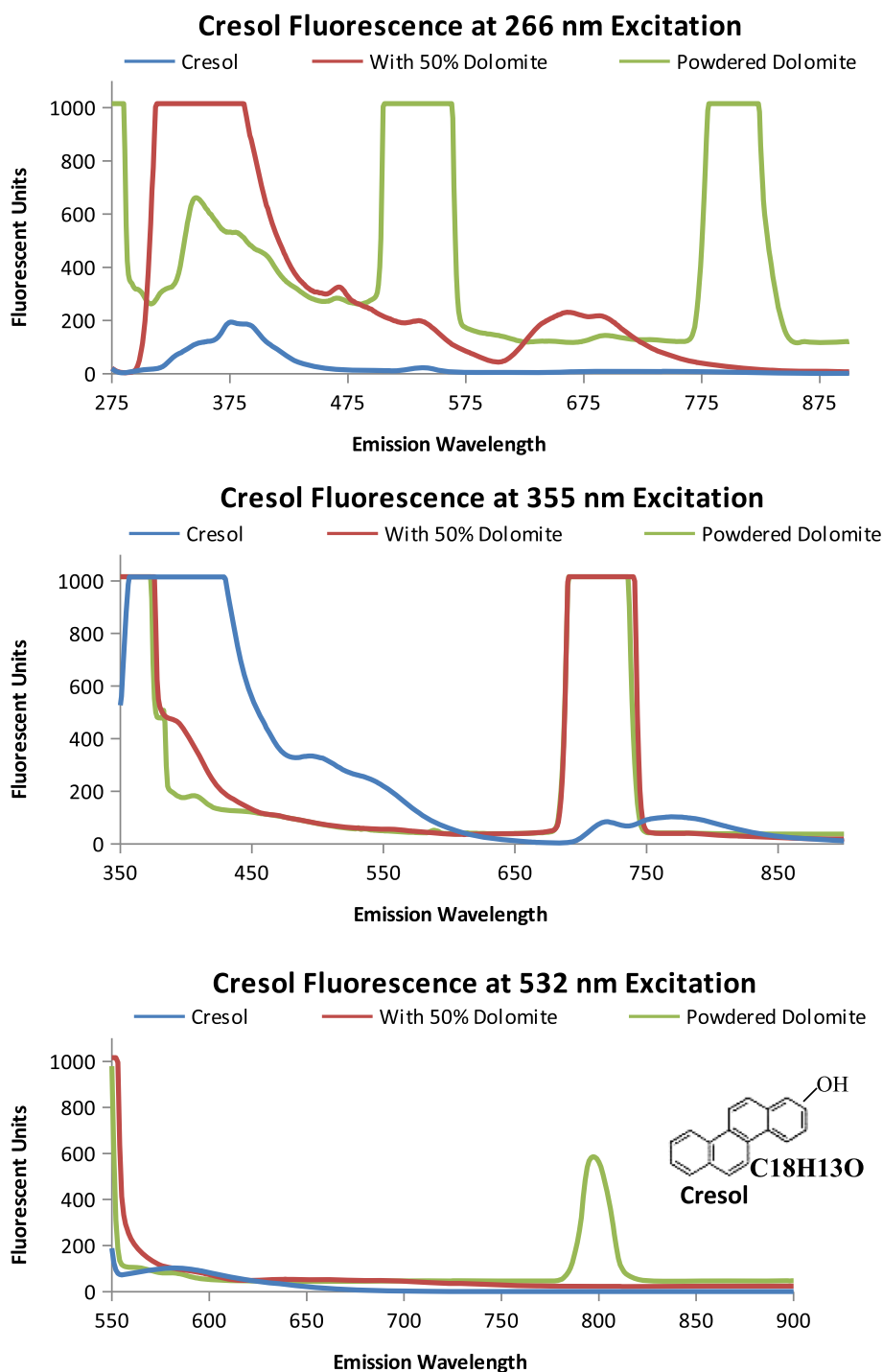


Figure 7 Cresol Fluorescence. Emission spectra of cresol, powdered dolomite, and a 50/50 mix when excited excitation wavelengths 266 nm, 355 nm, and 532 nm. The molecular structure and formula is shown on the 532 nm emission graph.

Naphthalene, as shown in Figure 5, also has an identifiable emission spectrum as pronounced by the 683 nm emission peak at 532 nm excitation. Naphthalene and Phenanthrene have similar spectrum profiles at 355 nm

excitation, the higher peak intensity at 818 nm distinguishes Phenanthrene from Naphthalene.

The Martian surface contains superoxides [39] and therefore, oxidized polycyclic aromatic hydrocarbons

(naphthol and cresol) were measured and compared to species without the addition of a hydroxyl group. As shown in Figure 6, naphthol, powdered dolomite, and the 50% naphthol, 50% dolomite by volume mixture have relatively similar emission spectrum. Some differences are the relative fluorescent units at 266 nm excitation and the naphthol emission peak at 355 nm excitation. Cresol, as shown in Figure 7, has a distinct emission spectrum for each excitation wavelength. At 266 nm excitation

the cresol spectrum has a less fluorescence than dolomite. At 355 nm Cresol has an enhanced fluorescence followed from 380 to 440 nm. At 532 nm the dolomite has an emission peak centered at 796 nm. The hydroxyl radical alters the emission spectrum of the PAHs, by reducing the fluorescence as seen between the Naphthalene and Naphthol in Figure 8.

We measured minerals known to be on the surface of Mars. Non-contact or remote mineral identification would

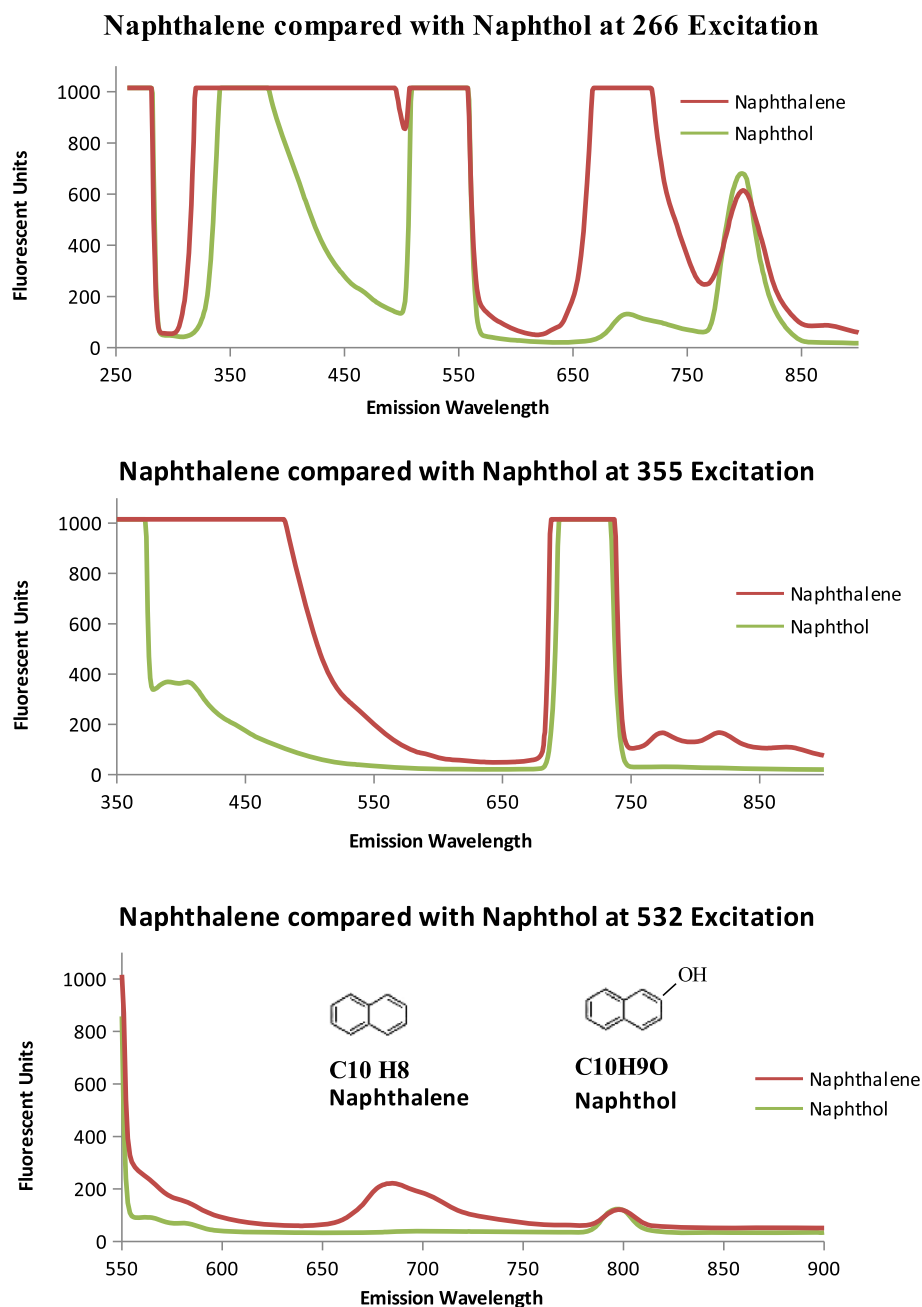
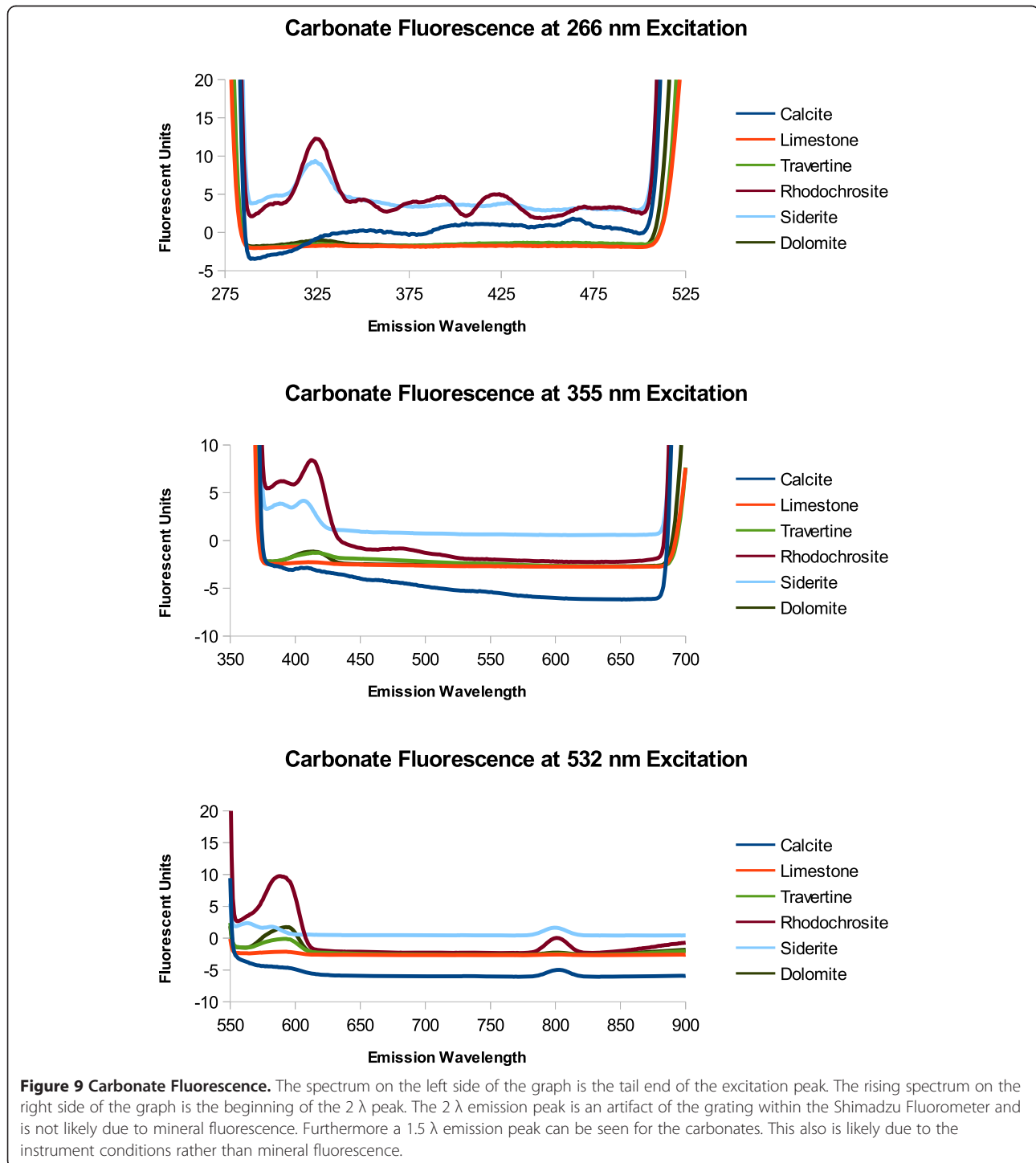


Figure 8 Naphthalene and Naphthol Fluorescence. Emission spectra of Naphthalene at 266 nm, 355 nm, and 532 nm compared with Naphthol to investigate the effect of a hydroxyl group. The molecular structure and formula is shown on the 532 nm emission graph for each molecule.

improve the scientific merit of the instrument. Also, as reported by Smith et al. [26] the detection of biomolecular fluorescence was influenced by mineral fluorescence. The data in Figure 9 shows the emission spectra of carbonates (calcite, limestone, travertine, rhodochrosite, siderite, and dolomite) and Figure 10 shows some water associated minerals (perchlorate, hematite (red and black), serpentine, and

jarosite), known to be on the surface of Mars, when excited at 266 nm, 355 nm, and 532 nm. The portion of the spectra graphed is from the tail end of the excitation peak to the beginning of the 2λ resonance fluorescence peak. Fluorescence beyond the 2λ peak is unexpected due to the large Stokes shift and lower energy output. At 266 nm excitation rhodochrosite, siderite, hematite, and perchlorate have



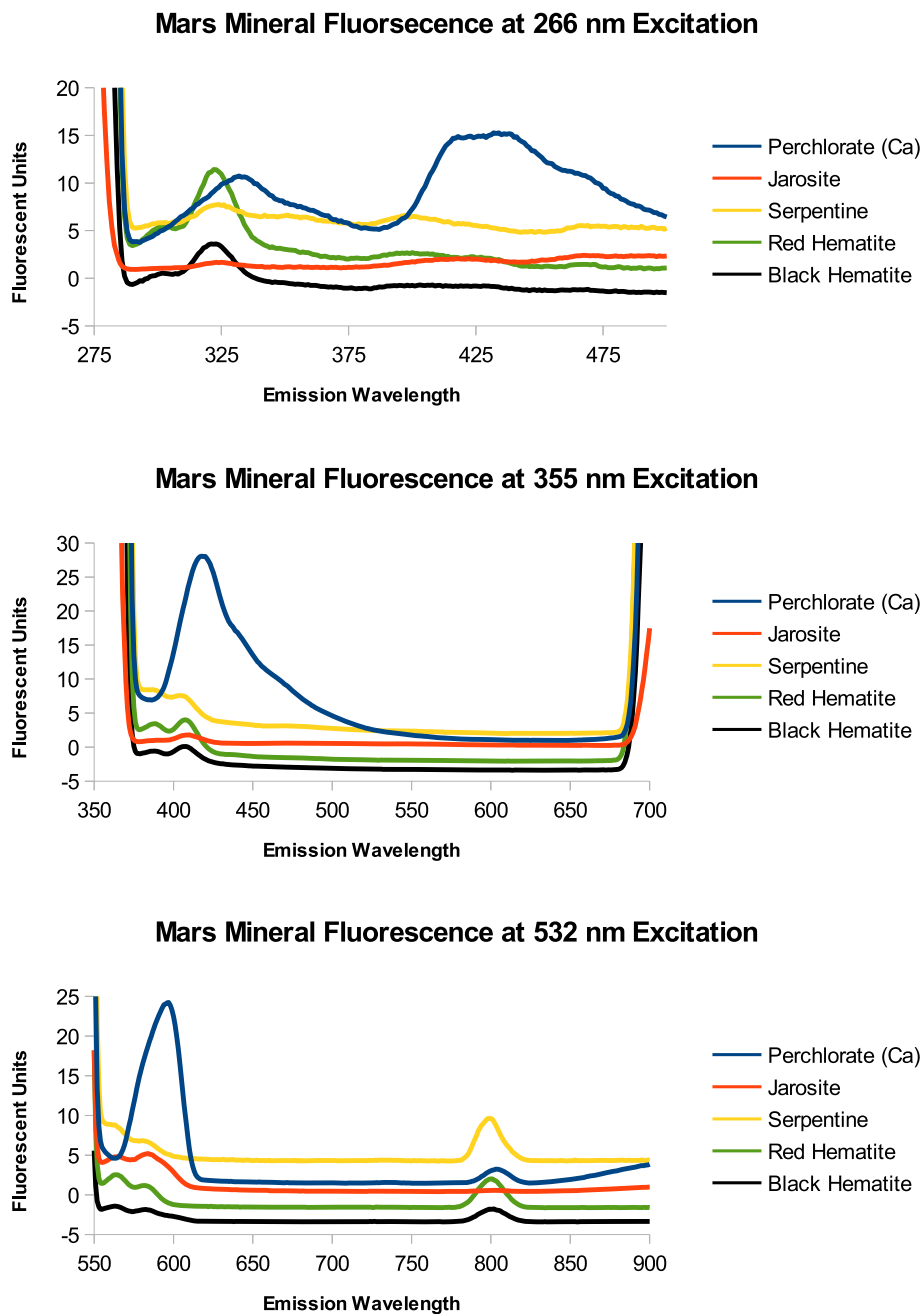


Figure 10 Fluorescence of Mars Minerals. The spectrum on the left side of the graph is the tail end of the excitation peak. The rising spectrum on the right side of the graph is the beginning of the 2λ peak. The 2λ emission peak is an artifact of the grating within the Shimadzu Fluorometer and is not likely due to mineral fluorescence. Furthermore a 1.5λ emission peak can be seen for Ca perchlorate. This also is likely due to the instrument conditions rather than mineral fluorescence.

Table 3 Biomolecules, organics, and minerals detectable by fluorescence by measuring the emission spectra, when excited at the corresponding wavelength

266 nm excitation	355 nm excitation	532 nm excitation
Adenosine Tri phosphate (ATP), Tryptophan, Tyrosine, Pyrene, Phenanthrene, Naphthalene, Mg Perchlorate, Hematite, Calcite, Siderite	Dipicolinic acid, NADH, Phenanthrene, Naphthol, Cresol, Mg Perchlorate, Siderite, Rhodochrosite, Hematite	Jarosite, Rhodochrosite, Dolomite, Naphthalene

distinct emission peaks. At 355 nm excitation, most minerals have a small fluorescence peak between 400 and 410 nm with the exception of perchlorate which fluoresces about fifty times brighter at 538 nm and 589 nm. At 532 nm the peaks are likely due to scattering of light or a grating effect at 1.5λ rather than fluorescence, except for the small emission peak at 726 nm from perchlorate.

Discussion

The survey of PAH and mineral fluorescence performed in this study illustrates that the 1064 nm laser available in the flight ready ChemCam instrument modified with the addition of the three frequency multipliers (266 nm, 355 nm, 532 nm) and band pass filters would provide an excellent site survey tool in near real time based on fluorescence measurements. Using mostly flight qualified hardware reduces the risk and cost associated with new instrumentation. A modified version of the ChemCam instrument described in this paper would be able to recognize biomolecules, PAHs, and minerals. Table 3 lists the material identifiable at the specified wavelengths.

With the operational flexibility of remote measurements, an outcrop could be surveyed a few meters away to avoid risks associated with movement. This greatly reduces the chance of mechanical failure from the rover getting stuck and expands the range of the target selection area. Future research will focus on expansion of the target database to include meteorites and tektites and on taking fluorescent measurements under conditions that are similar to those anticipated on Mars to determine the distances at which fluorescence detection is feasible.

Conclusions

We have developed a conceptual design for a fluorescence-based instrument for stand-off detection of organics on Mars. Our design is based on the technology developed for the ChemCam LIBS instrument that has been constructed for the Mars Science Laboratory mission. The key design change would be the addition of wavelength multiplexers to create higher harmonics of the 1064 nm laser that is presently on ChemCam. These lower wavelengths allow for fluorescence of both organic and mineral detection. To demonstrate this we have investigated the fluorescence properties at specific harmonic wavelengths of organics and minerals relevant to Mars. From this design work and data collection, our main conclusions are:

- 1) Fluorescence can be used to detect organics (PAH), and minerals that are expected to be on Mars.
- 2) The fluorescence instrument proposed is comprised almost entirely of flight-qualified Mars surface operational hardware reducing the risk and cost.

- 3) Feasibility of the instrument design offers a high scientific return (detection of organics) while expending minimal resources (time, development costs).
- 4) This instrument should be considered for the next mission to Mars as a site survey tool.

Additional file

Additional file 1: Table S1. Fluorometer Mineral List. Rocks analyzed using a custom rock holder in a Shimadzu 1501 fluorometer excited at 266 nm, 355 nm, and 532 nm. **Figure S1.** Varied Silica Content Emission Spectra. Igneous Rocks classified by silica content. Basalt has the lowest silica content, while Dacite has the highest. The middle silica content (Andesite) has the highest fluorescence. **Figure S2.** Sulfates Emission Spectra. Elemental sulfur compared with sulfate compounds. **Figure S3.** Oxides Emission Spectra. Ilmenite an TiO abundant at impact sites and on the Moon, compared with Pyrolusite a mineral that branches similar to trees, and Magnetite a known Mars mineral. **Figure S4.** Same Composition Emission Spectra. Fluorescence from three minerals with the same composition, but formed under different conditions.

Competing interests

The authors declare that they have no competing interests.

Authors' contributions

HDS prepared the samples and carried out the fluorescence measurements, participated in discussions of the instrument design, and drafted the manuscript. CPM advised on all aspects of the ChemCam Instrument, participated in data analysis and discussion, and drafted a manuscript section. AGD drafted two figures for the manuscript, participated in fluorescence measurements and instrument design discussion. RCS advised on the all aspects of this research, assisted in data analysis and discussions. AJA advised on and provided the supplies for the PAH, and participated in data interpretation and discussions. PRG advised on the mineralogy aspects of this research and participated in data interpretation and discussions. All authors read and approved the final manuscript.

Acknowledgment

The authors would like to thank Dr. Charlie Miller of the USU Biological and Irrigation Engineering department for use of the Shimadzu 1501 Fluorometer. Dr. John Shervais and Marlon Jean of the USU Geology Department for access to the mineralogy and petrology collection, and to Dr. Chris Lloyd for helpful discussions. CPM was supported through funding from the NASA Planetary Protection Program. HDS is grateful for the NASA Graduate Student Research Program and the Planetary Protection Program for funding this research.

Author details

¹Department of Biological Engineering, Utah State University, Logan, UT, USA. ²NASA Ames Research Center, Space Science Division, Moffett Field, CA, USA. ³Desert Sensors, Logan, UT 84341, USA. ⁴Department of Biology, Utah State University, Logan, UT, USA. ⁵Department of Plants, Soils and Climate, Utah State University, Logan, UT, USA.

Received: 8 January 2014 Accepted: 11 June 2014

Published: 1 July 2014

References

1. Wiens RC, Maurice S, Barraclough B, Saccoccio M, Barkley WC, Bell JF, Bender S, Bernardin J, Blaney D, Blank J, Bouye M, Bridges N, Bultman N, Cais P, Clanton RC, Clark B, Clegg S, Cousin A, Cremers D, Cros A, DeFlores L, Delapp D, Dingler R, D'Uston C, Dyar MD, Elliott T, Enemark D, Fabre C, Flores M, Forni O, et al: **The ChemCam instruments on the Mars Science Laboratory (MSL) rover: body unit and combined system performance.** *Space Sci Rev* 2012, **170**(1-4):167-227.
2. Angel SM, Gomer NR, Sharma SK, McKay C: **Remote Raman spectroscopy for planetary exploration: a review.** *Appl Spectrosc* 2012, **66**(2):137-150.

3. Sharma SK, Misra AK, Lucey PG, Wiens RC, Clegg SM: **Combined remote LIBS and Raman spectroscopy at 8.6 m of sulfur-containing minerals, and minerals coated with hematite or covered in basaltic dust.** *Spectrochim Acta A* 2007, **68**:1036–1045.
4. Storrie-Lombardi MC, Muller JP, Fisk MR, Griffiths AD, Coates AJ: **Potential for non-destructive astrochemistry using the ExoMars PanCam.** *Geophys Res Lett* 2008, **35**:L12201.
5. Hoge FE, Swift RN: **Airborne simultaneous spectroscopic detection of laser-induced water Raman backscatter and fluorescence from chlorophyll a and other naturally occurring pigments.** *Appl Opt* 1981, **20**(18):3197–3205.
6. Allamandola LJ, Sandford SA, Wopenka B: **Interstellar polycyclic aromatic hydrocarbons and carbon in interplanetary dust particles and meteorites.** *Science* 1987, **237**(4810):56–59.
7. Chyba CF, Thomas PJ, Brookshaw L, Sagan C: **Cometary delivery of organic molecules to the early Earth.** *Science* 1990, **249**(4967):366–373.
8. Flynn GJ: **The delivery of organic matter from asteroids and comets to the early surface of Mars.** *Earth Moon Planet* 1996, **72**(1–3):469–474.
9. Hoge FE, Wright CW, Kana TM, Swift RN, Yungel JK: **Spatial variability of oceanic phycoerythrin spectral types derived from airborne laser-induced fluorescence emissions.** *Appl Opt* 1998, **37**(21):4744–4749.
10. Karlitschek P, Lewitzka F, Bünting U, Niederkrüger M, Marowsky G: **Detection of aromatic pollutants in the environment by using UV-laser-induced fluorescence.** *Appl Phys B* 1998, **67**(4):497–504.
11. Ehrenfreund P, Charnley SB: **Organic molecules in the interstellar medium, comets, and meteorites: a voyage from dark clouds to the early Earth.** *Annu Rev Astron Astrophys* 2000, **38**(1):427–483.
12. Feldmann C, Jüstel T, Ronda CR, Schmidt PJ: **Inorganic luminescent materials: 100 years of research and application.** *Adv Funct Mater* 2003, **13**(7):511–516.
13. Sephton MA, Love GD, Watson JS, Verchovsky AB, Wright IP, Snape CE, Gilmour I: **Hydrolysis of insoluble carbonaceous matter in the Murchison meteorite: new insights into its macromolecular structure.** *Geochim Cosmochim Acta* 2004, **68**(6):1385–1393.
14. Gabrecht T: *Clinical Fluorescence Spectroscopy And Imaging For The Detection Of Early Carcinoma By Autofluorescence Bronchoscopy And The Study Of The Protoporphyrin Ix Pharmacokinetics In The Endometrium*; 2006. Doctorate Thesis École Polytechnique Fédérale De Lausanne.
15. Dartnell LR, Storrie-Lombardi MC, Ward JM: **Complete fluorescent fingerprints of extremophilic and photosynthetic microbes.** *Int J Astrobiol* 2010, **9**(4):245–257.
16. Sattler B, Storrie-Lombardi M, Foreman C, Tilg M, Psenner R: **Laser-induced fluorescence emission (LIFE) from Lake Fryxell (Antarctica) cryoconites.** *Ann Glaciol* 2010, **51**(56):145–152.
17. Cabrol NA, Cabrol NA, Wettergreen D, Warren-Rhodes K, Grin EA, Moersch J, Chong Diaz G, Cockell CS, Coppin P, Demergasso C, Dohm J, Ernst L, Fisher G, Glasgow J, Hardgrove C, Hock AN, Jonak D, Marinangeli L, Edwin Minkley E, Ori GG, Piatek J, Pudenz E, Smith T, Stubbs K, Thomas G, Thompson D, Waggoner A, Wagner M, Weinstein S, Wyatt M: **Life in the Atacama: searching for life with rovers (science overview).** *J Geophys Res* 2007, **112**:G04502. doi:10.1029/2006JG000298.
18. Bay RC, Bramall NE, Price PB: **Search for microbes and biogenic compounds in polar ice using fluorescence.** In *Life in Ancient Ice*. Edited by Castello JD, Rogers SO. New Jersey, USA: Princeton University Press; 2005:268–276.
19. Storrie-Lombardi MC, Sattler B: **Laser-induced fluorescence emission (LIFE): in-situ nondestructive detection of microbial life in the ice covers of Antarctic lakes.** *Astrobiology* 2009, **9**(7):659–672.
20. Bhartiya R, Salas EC, Hug WF, Reid RD, Lane AL, Edwards KJ, Nealon KH: **Label-free bacterial imaging with deep UV laser induced native fluorescence.** *Appl Environ Microbiol* 2010, **76**(21):7231–7237.
21. Smith HD, Powers LS, Duncan AG, Neary PL, Lloyd CR, Anderson AJ, Sims RC, McKay CP: **In-situ microbial detection in Mojave desert soil using native fluorescence.** *Astrobiology* 2012, **12**(3):247–257.
22. Bozlee BJ, Misra AK, Sharma SK, Ingram M: **Remote raman and fluorescence studies of mineral samples.** *Spectrochim Acta A* 2005, **61**:2342–2348.
23. Ming DW, Archer PD Jr, Glavin DP, Eigenbrode JL, Franz HB, Sutter B, Brunner AE, Stern JC, Freissinet C, McAdam AC, Mahaffy PR, Cabane M, Coll P, Campbell JL, Atreya SK, Niles PB, Bell JF 3rd, Bish DL, Brinckerhoff WB, Buch A, Conrad PG, Des Marais DJ, Ehlmann BL, Fairén AG, Farley K, Flesch GJ, Francois P, Gellert R, Grant JA, Grotzinger JP, et al: **Volatile and organic compositions of sedimentary rocks in Yellowknife Bay, Gale Crater, Mars.** *Science* 2013, **342**:1245267–1–r. Published online 9 December. doi:10.1126/science.1245267.
24. Smith PH, Tampari LK, Arvidson RE, Bass D, Blaney D, Boynton WW, Carswell A, Catling DC, Clark BC, Duck T, DeJong E, Fisher D, Goetz W, Gunnlaugsson HP, Hecht MH, Hipkin V, Hoffman J, Hviid SF, Keller HU, Kounaves SP, Lange CF, Lemmon MT, Madsen MB, Markiewicz WJ, Marshall J, McKay CP, Mellon MT, Ming DW, Morris RV, Pike WT, et al: **H₂O at the Phoenix landing site.** *Science* 2009, **325**:58–61.
25. Griffiths AD, Coates AJ, Josset JL, Paar G, Hofmann B, Rueffer P, Pillinger CT, Sims MR, Pullan D: **The Beagle 2 stereo camera system: scientific objectives and design characteristics.** *Planet Space Sci* 2005, **53**(14–15):1466–1482.
26. Griffiths AD, Coates AJ, Jaumann R, Michaelis H, Paar G, Barnes D, Josset JL, Team PC: **Context for the ESA ExoMars rover: the Panoramic Camera (PanCam) instrument.** *Int J Astrobiol* 2006, **5**(3):269.
27. McKay DS, Gibson EK, Thomas-Keprta KL, Hojatollah V, Romanek CS, Clemett SJ, Chillier XDF, Maechling CR, Zare RN: **Search for past life on Mars: possible relic biogenic activity in Martian meteorite ALH84001.** *Science* 1996, **273**:924–930.
28. Kuan YJ, Charnley SB, Huang HC, Tseng WI, Zbigniew K: **Interstellar glycine.** *Astrophys J* 2003, **593**(2):848–867. doi:10.1086/375637.
29. Smith HD, Powers LS, Duncan AG, Neary PL, Anderson AJ, Sims RC, McKay CP: *In Situ Microbial Detection in the Mojave Desert Using Native Fluorescence*; 2010. Utah State University, Department of Biological Engineering, PhD Dissertation.
30. Katayama M, Matsuda Y, Shimokawaa KI, Tanabea S, Kanekob S, Harac I, Satoc H: **Simultaneous determination of six adenylyl purines in human plasma by high-performance liquid chromatography with fluorescence derivatization.** *J Chromatogr B Biomed Sci Appl* 2001, **760**(1):53–58.
31. Seaver M: **Size and fluorescence measurements for field detection of biological aerosols.** *Aerosol Sci Technol* 1999, **30**(2):174–185.
32. Richards-Kortum R, Sevick-Muraca E: **Quantitative optical spectroscopy for tissue diagnosis.** *Annu Rev Phys Chem* 1996, **47**:555–606.
33. Nevin A, Cather S, Anglos D, Fotakis C: **Laser-induced fluorescence analysis of protein-based binding media.** In *Lasers in the Conservation of Artworks, Volume 116*. Edited by Nimrichter J, Kautek W, Schreiner M: Springer Proceedings in Physics; 2007:399–406.
34. Alimova A, Katz A, Savage HE, Shah M, Minko G, Will DE, Rosen RB, McCormick SA, Alfano RR: **Native fluorescence and excitation spectroscopic changes in *Bacillus subtilis* and *Staphylococcus aureus* bacteria subjected to conditions of starvation.** *Appl Opt* 2003, **42**:19.
35. Kuijt J, García-Ruiz C, Stroomborg GJ, Marina ML, Ariese F, Brinkman UAT, Gooijer C: **Laser-induced fluorescence detection at 266 nm in capillary electrophoresis polycyclic aromatic hydrocarbon metabolites in biota.** *J Chromatogr A* 2001, **907**:291–299.
36. Pujari SR, Bosale PN, Rao PMR: **Sensitized monomer fluorescence and excitation energy transfer in perylene-doped phenanthrene in crystalline and polymer matrix.** *Mater Res Bull* 2002, **37**:439–448.
37. Wilson JN, Gao J, Koo ET: **Oligodeoxyfluorosides: strong sequence dependence of fluorescence emission.** *Tetrahedron* 2007, **63**(17):3427–3433.
38. Shimadzu Corporation: *RF-1501 Spectrophotometer*; 2003.
39. Klein HP: **The Viking biological investigation: general aspects.** *J Geophys Res* 1977, **82**(28):4677–4680.

doi:10.1186/1754-1611-8-16

Cite this article as: Smith et al.: An instrument design for non-contact detection of biomolecules and minerals on Mars using fluorescence. *Journal of Biological Engineering* 2014 **8**:16.